PROTEINS
STRUCTURE ■ FUNCTION ■ BIOINFORMATICS

STRUCTURE NOTE

Structure of the yeast Bre1 RING domain

Pankaj Kumar and Cynthia Wolberger*

Department of Biophysics and Biophysical Chemistry, Johns Hopkins University School of Medicine, 725 North Wolfe Street, Baltimore, Maryland, 21205

ABSTRACT

Monoubiquitination of histone H2B at Lys123 in yeast plays a critical role in regulating transcription, mRNA export, DNA replication, and the DNA damage response. The RING E3 ligase, Bre1, catalyzes monoubiquitination of H2B in concert with the E2 ubiquitin-conjugating enzyme, Rad6. The crystal structure of a *C*-terminal fragment of Bre1 shows that the catalytic RING domain is preceded by an *N*-terminal helix that mediates coiled-coil interactions with a crystallographically related monomer. Homology modeling suggests that the human homologue of Bre1, RNF20/RNF40, heterodimerizes through similar coiled-coil interactions.

Proteins 2015; 83:1185–1190.

Key words: X-ray crystallography; ubiquitin; E2 ubiquitin-conjugating enzyme; histone modification; transcription.

INTRODUCTION

The attachment of the 76-amino acid protein, ubiquitin, to substrate lysines regulates a vast array of biological processes. In addition to its well-known role in targeting proteins for proteasomal degradation, ubiquitination plays nondegradative signaling roles in transcription regulation, endosomal sorting, and the DNA damage response. Ubiquitination of proteins initiates with the ATP-dependent activation of ubiquitin (Ub) by a ubiquitin-activating enzyme (E1), resulting in a thioester linkage between the *C*-terminus of ubiquitin and the active site cysteine of E1. The activated ubiquitin is transferred to the active site cysteine of ubiquitin-conjugating enzyme E2 in a transthiolation reaction, generating an E2∼Ub conjugate.[1] The E3 ligase binds to the E2∼Ub conjugate as well as to the substrate and facilitates transfer of ubiquitin to the substrate, where ubiquitin is covalently linked to the ε-amino group of lysine or, in some cases, to the protein *N*-terminus. E3 ligases function by two general mechanisms:[2] they either serve as a catalytic intermediate in ubiquitination, as in the case of homologous to E6AP carboxyl terminus (HECT)-type E3 ligases, or they mediate transfer of ubiquitin directly from the E2∼Ub thioester to substrate, as in the case for really interesting new gene (RING)-type E3 ligases. Structural studies have shown that the RING domain binds to the E2 enzyme and positions the donor ubiquitin in the E2∼Ub conjugate for ubiquitin transfer.[3–5]

Different RING E3 ligases function as monomers, dimers, or heterodimers. There are monomeric RING finger E3 ligases, including Mdm2[6] and c-Cbl.[7] Homodimeric RING E3 ligases such as cIAP2,[8] RNF4 (RING

Grant sponsor: National Institute of General Medical Sciences; grant numbers: GM-095822; AGM-12006; Grant sponsor: National Cancer Institute; grant number: ACB-12002; Grant sponsor: Advanced Photon Source; grant number: DE-AC02-06CH11357.

*Correspondence to: Cynthia Wolberger; Department of Biophysics and Biophysical Chemistry, Johns Hopkins University School of Medicine, 725 North Wolfe Street, Baltimore, MD, 21205. E-mail: cwolberg@jhmi.edu
Received 8 December 2014; Revised 31 March 2015; Accepted 5 April 2015
Published online 9 April 2015 in Wiley Online Library (wileyonlinelibrary.com).
DOI: 10.1002/prot.24812

finger protein 4),[9] RNF8 [10] and Rad18 [11] dimerize through the core RING domain and, in some cases, through flanking regions located at either the *N*-terminus or *C*-terminus of the core RING motif. In some cases, dimerization is required for catalytic function: RNF4, for example, functions as an obligate dimer, and mutations that disrupt dimerization also disrupt E3 ligase activity.[9] Some RING E3 ligases are heterodimers, such as BRCA1 (breast cancer-associated 1), which functions as a heterodimer with BARD1 (BRCA1-associated RING domain 1).[12] In this case, one RING domain (BARD1) lacks E3 ligase activity but is thought to stabilize the active E2-binding (BRCA1) RING domain.[12]

Bre1 from yeast and its human homologue, RNF20/40, are RING E3 ligases that catalyze monoubiquitination of histone H2B[15,16] in conjunction with the E2 ubiquitin-conjugating enzyme, Rad6.[17] Monoubiquitination of H2B-K123 in yeast (H2B-K120 in human cells)[18] is enriched in highly transcribed regions, where it is required for subsequent methylation of histone H3-K4 [19] and for recruiting the H2A/H2B chaperone, FACT, which facilitates transcription through chromatin.[20] H2B-K123/K120 monoubiquitination has also been implicated in regulating DNA replication,[21] the DNA damage response[22] and mRNA splicing.[23] Yeast Bre1 forms a homodimer through intermolecular associations of both an *N*-terminal region (residues 1–110) and a *C*-terminal region (residues 450-700).[24] The RING domain of Bre1, located at the *C*-terminus of the 700-residue Bre1 protein, is crucial for mono-ubiquitination of histone H2B,[14,15] as is the dimerization region.[24] To provide insights into Bre1 structure and dimerization, we carried out structural and solution studies of a fragment of a *C*-terminal fragment of yeast Bre1-spanning residues 591-700, which contains the RING domain and a predicted coiled-coil region.

MATERIALS AND METHODS

Cloning

The DNA sequence encoding the *C*-terminal fragment of Bre1 spanning residues 591-700 was amplified by polymerase chain reaction (PCR) from a *Saccharomyces cerevisiae* cDNA library and cloned into a pET32a vector containing an *N*-terminal thioredoxin-hexahistidine (TRX-His_6) tag followed by a tobacco etch virus (TEV) protease cleavage site**.** The Bre1 (591-700) W655R mutant was generated using the Q5 site-directed mutagenesis kit (New England Biolabs) and verified by DNA sequencing.

Protein expression and purification

E.coli Rosetta2 DE3 pLysS cells were transformed with the plasmid encoding wild-type or mutant Bre1 residues 591-700. Cells were grown at 37 °C in Luria-Bertani (LB) medium supplemented with 50 μ*M* $ZnCl_2$ to an $OD_{600\ nm}$ of ~0.6, induced with 0.25 m*M* isopropyl-β-*D*-1-thiogalactopyranoside (IPTG) and grown overnight at 18 °C before harvesting by centrifugation. Cells were lysed by sonication in buffer containing 50 m*M* Tris, pH 7.5, 300 m*M* sodium chloride, 50 μ*M* $ZnCl_2$, 1 m*M* phenylmethanesulfonylfluoride (PMSF), and 5–10 μ*M* each of leupeptin, aprotinin, and pepstatin protease inhibitors. The whole-cell lysate was clarified by centrifugation, and the supernatant was passed through a 5 mL HisTrap HP (GE Healthcare Life Sciences) nickel affinity column pre-equilibrated with buffer containing 50 m*M* Tris, pH 7.5, 300 m*M* sodium chloride, 50 μ*M* $ZnCl_2$, 20 m*M* imidazole, and 0.1 m*M* PMSF. After washing the column with 25 column volumes of loading buffer, the protein was eluted with a gradient of loading buffer plus 1–1000 m*M* imidazole. The TRX-His_6 tag was removed from the Bre1 RING by incubation with 1 mg of tobacco etch virus (TEV) protease overnight during dialysis at 4 °C against buffer containing 50 m*M* Tris, pH 7.5, 150 m*M* sodium chloride, 50 μ*M* $ZnCl_2$, and 0.1 m*M* PMSF. Directly after the TRX-His_6 tag cleavage with TEV protease, protein was purified with a HiTrap SP-XL cation-exchange column (GE Healthcare Life Sciences) to remove the TRX-His_6 and uncleaved tagged protein. The purified protein was concentrated to 21 mg/mL, flash-frozen in liquid nitrogen and stored at −80 °C until use.

Size-exclusion chromatography

Purified Bre1(591-700) wild-type or mutant (W655R) protein at a concentration of 25 mg/mL was run at 0.5 mL/min on a Superdex 75 10/300 column (GE Healthcare Life Sciences) pre-equilibrated with 50 m*M* Tris, pH 7.5, 150 m*M* NaCl, 50 μ*M* $ZnSO_4$, and 1 m*M* tris(2-carboxyethyl)phosphine (TCEP).

Crystallization and structure determination

Bre1 crystals of approximate dimensions 0.25 mm × 0.15 mm × .05 mm were obtained by the hanging-drop vapor diffusion method at 20 °C by mixing 2.0 μL of protein solution with 2.0 μL of a reservoir solution containing 2.0 *M* ammonium sulfate and 0.1 m*M* sodium acetate, pH 5.2. The crystals were transferred to a cryoprotectant solution containing reservoir solution supplemented with 30% glycerol and then flash-frozen.

Diffraction data were collected using synchrotron radiation (1.0 Å wavelength) at the Advanced Photon Source (APS) GM/CA CAT beamline 23-ID-D and recorded with a PILATUS3 detector. Diffraction data were processed using HKL3000.[25] The crystals belong to primitive hexagonal space group $P6_122$ with one monomer in the asymmetric unit. The crystal structure was solved by the molecular replacement method using the program, PHASER-MR[26] in the Phenix suite of programs,[27] using the coordinates of the RING1B RING domain from the

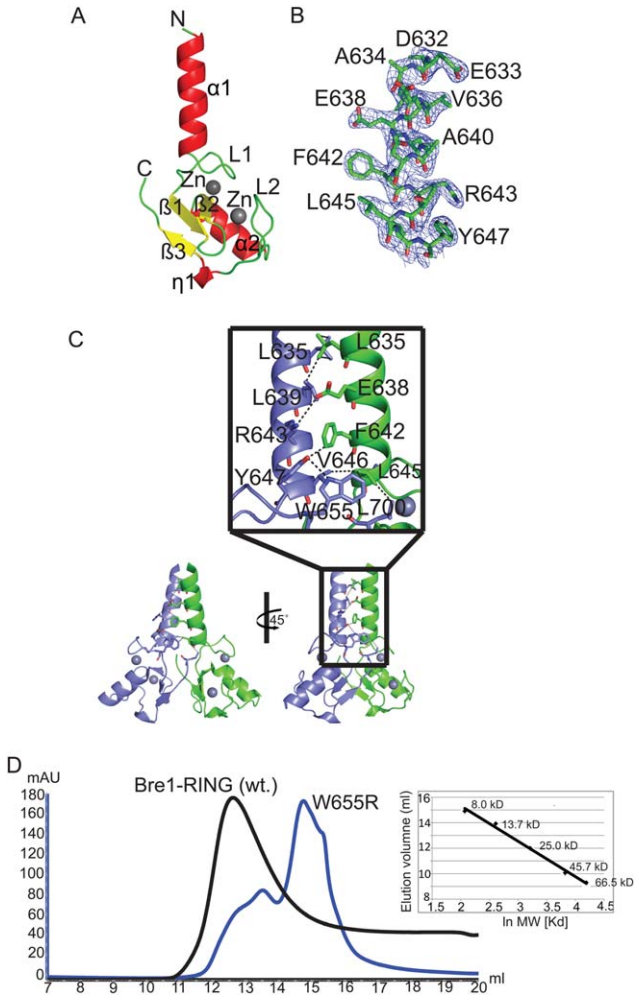

Figure 1

Crystal structure of the Bre1 RING domain**. (A)** Structure of the Bre1 monomer (632-700) with secondary structure elements and zinc atoms labeled. **(B).** *N*-terminal Bre1 residues, 632-647, with corresponding 2Fo-Fc electron density maps contoured at 1.0 σ. **(C)** Crystallographic dimer formed by the Bre1 *C*-terminal RING fragment. Inset shows the set of side chain interactions mediated by the *N*-terminal helices and the RING domain. **(D)** Size-exclusion chromatography showing that the 12.5 kDa *C*-terminal Bre1 RING wild-type fragment migrates as a dimer on a Superdex 75 10/300 column, while the W655R mutation disrupts the RING dimer. Inset shows column calibration.

structure of the RING1B-BMI1 heterodimer[28] (Protein Data Bank (PDB) code 2CKL) as a search model. The initial solution was subjected to multiple rounds of crystallographic refinement with the phenix.refine program in the Phenix suite of programs[29] followed by model building to the electron density with COOT[30] to yield the structure of the Bre1 RING domain. Bre1 residues 632-647, which are *N*-terminal to the RING domain, were manually built into 2Fo-Fc electron density maps contoured at 1.0 σ (Fig. 1B). Residues 591-631 are disordered as judged by the absence of electron density. The final model contains residues 632-700 of Bre1 and 9 water molecules, with an *R* factor of 22.05% and an R_{free} of 24.73% for all data between 26.2 and 2.25 Å resolution. Figures were prepared with PyMol Molecular Graphics System, Version 1.5.0.4 Schrödinger, LLC. Coordinates and diffraction data have been deposited in the PDB under accession code 4R7E.

Homology modeling of human RNF20 (residues 906-974) and RNF40 (residues 932-1000) was performed with SWISS-MODEL[31] using the Bre1 RING structure as a template. The structures were further refined using Chiron.[32]

RESULTS AND DISCUSSION

Bre1 is a dimeric RING domain with an *N*-terminal coiled coil

The structure of a *C*-terminal fragment of Bre1 spanning residues 632-700 and containing the RING domain was determined at 2.25 Å resolution. Data collection and refinement statistics are summarized in Table I. Although the crystallized fragment also included residues 591-631, there is no corresponding electron density, indicating that this region is disordered. The Bre1 monomer contains a RING motif (residue 647-700) flanked by an *N*-terminal α-helix (α1) (Fig. 1A). Figure 1B shows residues 632-647 from *N*-terminal α-helix (α1) manually built

Table I

Data Collection and Refinement Statistics

Space group and unit cell	
Space group	$P6_122$
Unit cell	
a, b, c (Å)	56.77, 56.77, 134.86
Data-processing statistics	
Beamline	APS 23-ID-D
Wavelength (Å)	1.000
Resolution (Å)[a]	26.16–2.25 (2.33–2.25)
Total/Unique reflections	11395 6530
Completeness (%)[a]	98.85 (100.0)
R_{merge} (%)[a]	9.2 (38.5)
Mean I/σ (I)[a]	24.39 (3.34)
Refinement Statistics	
Resolution (Å)	26.16–2.25
R_{work} (%)	22.05
R_{free} (%)	24.73
rms deviation	
Bond lengths (Å)	0.01
Bond angles (Å)	1.24
Ramachandran plot (%)	
Most favored	98.51
Additionally allowed	1.49
Disallowed	0.0
Number of nonhydrogen atoms	
Protein	539
Water molecules	9
Average B-values (Å^2)	
Protein	74.4
Ligands	74.9

[a]Values in parenthesis are for the highest resolution shell.

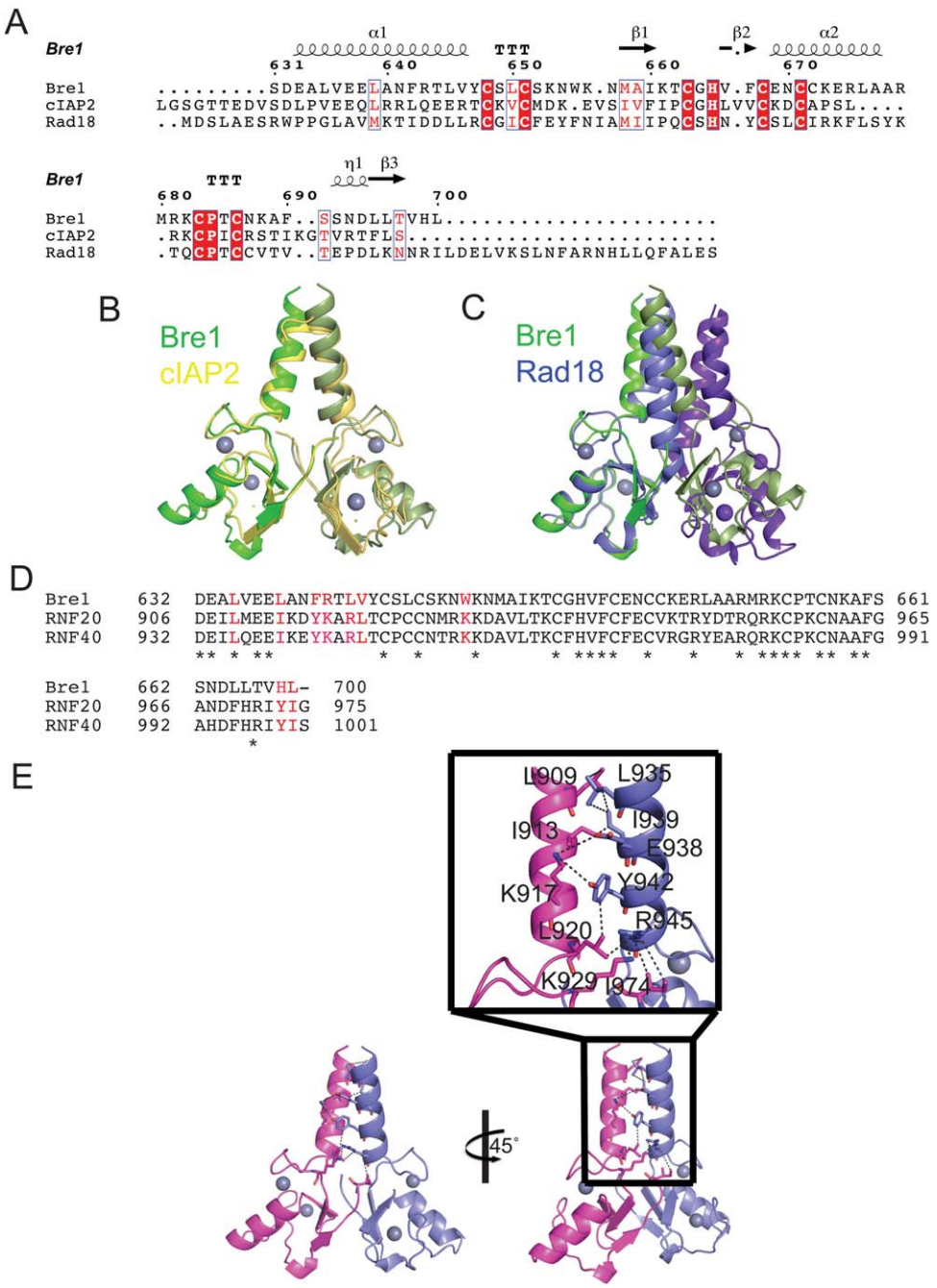

Figure 2

Comparison of the Bre1 RING dimer with human cIAP2, Rad18 and RNF20/40**. (A)** Sequence alignment of Bre1 with human cIAP2 and Rad18 RING domains. Residues in red indicate sequence similarity and a red box denotes sequence identity. **(B)** Superposition of Bre1 (bright green and pea green) with cIAP2 (yellow and yellow-orange; PDB ID 3EB5). **(C)** Superposition of Bre1 (bright green and pea green) and RAD18 (blue and purple blue; PDB ID 2Y43) dimers. **(D)**. Sequence alignment of Bre1 and human RNF20, RNF40. Asterisks (*) indicate sequence identity between Bre1, RNF20 and RNF40. Red residues are involved in dimerization of the Bre1 C-terminal RING fragment. **(E)** Model of the RNF20 (magenta)/RNF40 (blue) heterodimer. The inset shows details of the modeled interaction between RNF20 and RNF40.

into a 2Fo-Fc electron density map contoured at 1.0 σ. The core RING motif adopts a characteristic RING fold comprising a three-stranded antiparallel β-sheet (β1 from 657-660, β2 from 664-667, β3 from 695-697), a central α-helix (α2) and a 3_{10} helix (η1) (Fig. 1A). There are two long loops, loop1 (L1) from 647-657 and loop2 (L2) from 679-691, that are stabilized by coordination of two zinc ions within a C_3HC_4 cross-brace motif (Fig. 1A).

RING domain proteins can be either monomers or dimers, with RING dimerization in some cases important

for activity.[13] Although Bre1 crystallizes with one monomer in the asymmetric unit, a second monomer related by the crystallographic twofold axis gives rise to a Bre1 dimer with a total interface of 1031 Å^2 as calculated with PISA.[33] The dimerization interface consists of symmetric interactions between the two RING domains and coiled-coil interactions between the *N*-terminal α-helices (α1), where Leu 635, Leu 639, Phe 642, Leu 645, Val 646, Tyr 647, Trp 655, and Leu 700 are involved in hydrophobic interactions (Fig. 1C). Glu 638 and Arg 643 are in a position to form electrostatic interactions between opposing monomers given small adjustments to side-chain rotamers, suggesting that these residues may form a salt bridge in solution. To test whether the observed Bre1 crystallographic dimer reflects the solution state, we used size-exclusion chromatography and confirmed that Bre1 (591-700) migrates as an apparent dimer (Fig. 1D). By contrast, a mutant Bre1 protein containing a substitution predicted to disrupt the dimer interface, Trp655 to arginine, migrates primarily as a monomer (Fig. 1D), with just a small amount migrating as the wild-type dimer.

Comparison with other RING domain proteins

Comparisons with other dimeric RING E3 ligases show that the Bre1 RING dimer most closely resembles cIAP2,[8] which also contains an *N*-terminal helix [Figs. 2(A,B)]. The Bre1 RING dimer superimposes with the cIAP2 RING dimer with a root mean square difference (rmsd) of 1.3 Å. The relative orientation of the respective RING domains and the *N*-terminal coiled-coil align quite well despite the lack of sequence conservation between Bre1 and cIAP2. By contrast, RING domains such as human Rad18 [11] that dimerize via four-helix bundles are positioned differently as compared to Bre1 or cIAP2 (Fig. 2C), thus giving rise to a larger rmsd of 2.2 Å when the Bre1 and Rad18 RING dimers are superimposed. In Rad18, the RING domain is flanked by both *N*- and *C*-terminal helices that mediate dimerization with the helices from an opposing monomer, forming a four-helix bundle (Fig. 2C). Intact Bre1 lacks a *C*-terminal helix, as the present structure (Fig. 1C) is of a Bre1 fragment that extends to the protein *C*-terminal residue, Leu 700, which is ordered and is part of the RING domain (Fig. 1A). The relation between RING domains in the Bre1 and cIAP2 dimers is surprisingly different from that in Rad18 (Fig. 2C), suggesting that the different dimer interfaces may govern the relation between RING domains in a given dimer.

Model of human rnf20/40 heterodimer

The human homolog of yeast Bre1 is RNF20/RNF40, a heterodimeric E3 ligase.[16] The sequence of the helix—RING fragment of Bre1 from the present study is 43% similar to analogous regions of both RNF20 and RNF40 (Fig. 2D). In particular, most of the residues involved in dimerization at the *N*-terminal α-helical region of Bre1 RING are identical or similar to the RNF20/40 residues (Fig. 2E). To compare the dimerization of the human RNF20/40 RING heterodimer with the yeast Bre1 homodimer, we generated a homology model using SWISS-MODEL.[31] The Bre1 RING monomer was used as a template for each monomer, and the heterodimer interface was then generated based on the Bre1 homodimer (Fig. 2E). Overall, the RNF20/40 RING heterodimer preserves many of the key features of the Bre1 homodimer interface (Figs. 1D and 2E), including most of the hydrophobic interactions and the salt bridge.

CONCLUSION

Bre1 is an E3 ligase enzyme from *Saccharomyces cerevisiae* that catalyzes monoubiquitination of histone H2B and is similar to its human homolog, the RNF20/40 heterodimer. Our structural study shows that a *C*-terminal fragment of yeast Bre1 RING forms a homodimer through symmetrical interaction medicated by *N*-terminus helices and RING core motif. This structure provided the basis for homology modeling studies suggesting that the human RNF20/40 RING E3 ligase forms a heterodimer similar to that of yeast Bre1. Our study provides the first step toward a structural understanding of RING–RING interactions in yeast Bre1 and its human homologs.

ACKNOWLEDGMENTS

The authors thank Ming Yan for his help and advice.

REFERENCES

1. Ye Y, Rape M. Building ubiquitin chains: E2 enzymes at work. Nat Rev Mol Cell Biol 2009;10:755–764.
2. Berndsen CE, Wolberger C. New insights into ubiquitin E3 ligase mechanism. Nat Struct Mol Biol 2014;21:301–307.
3. Plechanovova A, Jaffray EG, Tatham MH, Naismith JH, Hay RT. Structure of a RING E3 ligase and ubiquitin-loaded E2 primed for catalysis. Nature 2012;489:115–120.
4. Dou H, Buetow L, Sibbet GJ, Cameron K, Huang DT. BIRC7-e2 ubiquitin conjugate structure reveals the mechanism of ubiquitin transfer by a RING dimer. Nat Struct Mol Biol 2012;19:876–883.
5. Scott DC, Sviderskiy VO, Monda JK, Lydeard JR, Cho SE, Harper JW, Schulman BA. Structure of a RING E3 trapped in action reveals ligation mechanism for the ubiquitin-like protein nedd8. Cell 2014; 157:1671–1684.
6. Linke K, Mace PD, Smith CA, Vaux DL, Silke J, Day CL. Structure of the MDM2/MDMX RING domain heterodimer reveals dimerization is required for their ubiquitylation in trans. Cell Death Differ 2008;15:841–848.
7. Zheng N, Wang P, Jeffrey PD, Pavletich NP. Structure of a c-Cbl-UbcH7 complex: RING domain function in ubiquitin-protein ligases. Cell 2000;102:533–539.

8. Mace PD, Linke K, Feltham R, Schumacher FR, Smith CA, Vaux DL, Silke J, Day CL. Structures of the cIAP2 RING domain reveal conformational changes associated with ubiquitin-conjugating enzyme (E2) recruitment. J Biol Chem 2008;283:31633–31640.
9. Liew CW, Sun H, Hunter T, Day CL. RING domain dimerization is essential for RNF4 function. Biochem J, 2010;431:23–29.
10. Zhang X, Chen J, Wu M, Wu H, Arokiaraj AW, Wang C, Zhang W, Tao Y, Huen MS, Zang J. Structural basis for role of ring finger protein RNF168 RING domain. Cell Cycle 2013;12:312–321.
11. Huang A, Hibbert RG, de Jong RN, Das D, Sixma TK, Boelens R. Symmetry and asymmetry of the RING-RING dimer of RAD18. J Mol Biol 2011;410:424–435.
12. Brzovic PS, Rajagopal P, Hoyt DW, King MC, Klevit RE. Structure of a BRCA1-BARD1 heterodimeric RING-RING complex. Nat Struct Biol 2001;8:833–837.
13. Plechanovova A, Jaffray EG, McMahon SA, Johnson KA, Navratilova I, Naismith JH, Hay RT. Mechanism of ubiquitylation by dimeric RING ligase RNF4. Nat Struct Mol Biol 2011;18:1052–1059.
14. Hwang WW, Venkatasubrahmanyam S, Ianculescu AG, Tong A, Boone C, Madhani HD. A conserved RING finger protein required for histone H2B monoubiquitination and cell size control. Mol Cell, 2003;11:261–266.
15. Wood A, Krogan NJ, Dover J, Schneider J, Heidt J, Boateng MA, Dean K, Golshani A, Zhang Y, Greenblatt JF, Johnston M, Shilatifard A. Bre1, an E3 ubiquitin ligase required for recruitment and substrate selection of rad6 at a promoter. Mol Cell 2003;11:267–274.
16. Kim J, Hake SB, Roeder RG. The human homolog of yeast Bre1 functions as a transcriptional coactivator through direct activator interactions. Mol Cell 2005;20:759–770.
17. Robzyk K, Recht J, Osley MA. Rad6-dependent ubiquitination of histone H2B in yeast. Science 2000;287:501–504.
18. Jung I, Kim SK, Kim M, Han YM, Kim YS, Kim D, Lee D. H2B monoubiquitylation is a 5'-enriched active transcription mark and correlates with exon-intron structure in human cells. Genome Res 2012;22:1026–1035.
19. Lee JS, Shukla A, Schneider J, Swanson SK, Washburn MP, Florens L, Bhaumik SR, Shilatifard A. Histone crosstalk between H2B monoubiquitination and H3 methylation mediated by COMPASS. Cell 2007;131:1084–1096.
20. Pavri R, Zhu B, Li G, Trojer P, Mandal S, Shilatifard A, Reinberg D. Histone H2B monoubiquitination functions cooperatively with FACT to regulate elongation by RNA polymerase II. Cell 2006;125:703–717.
21. Trujillo KM, Osley MA. A role for H2B ubiquitylation in DNA replication. Mol Cell 2012;48:734–746.
22. Wu J, Huen MS, Lu LY, Ye L, Dou Y, Ljungman M, Chen J, Yu X. Histone ubiquitination associates with BRCA1-dependent DNA damage response. Mol Cell Biol 2009;29:849–860.
23. Shieh GS, Pan CH, Wu JH, Sun YJ, Wang CC, Hsiao WC, Lin CY, Tung L, Chang TH, Fleming AB. H2B ubiquitylation is part of chromatin architecture that marks exon-intron structure in budding yeast. BMC Genomics 2011;12:627
24. Kim J, Roeder RG. Direct Bre1-Paf1 complex interactions and RING finger-independent Bre1-rad6 interactions mediate histone H2B ubiquitylation in yeast. J Biol Chem 2009;284:20582–20592.
25. Minor W, Cymborowski M, Otwinowski Z, Chruszcz M. HKL-3000: the integration of data reduction and structure solution–from diffraction images to an initial model in minutes. Acta Crystallogr D Biol Crystallogr 2006;62:859–866.
26. Read RJ. Pushing the boundaries of molecular replacement with maximum likelihood. Acta Crystallogr D Biol Crystallogr 2001;57:1373–1382.
27. Adams PD, Afonine PV, Bunkoczi G, Chen VB, Davis IW, Echols N, Headd JJ, Hung LW, Kapral GJ, Grosse-Kunstleve RW, McCoy AJ, Moriarty NW, Oeffner R, Read RJ, Richardson DC, Richardson JS, Terwilliger TC, Zwart PH. PHENIX: a comprehensive python-based system for macromolecular structure solution. Acta Crystallogr D Biol Crystallogr 2010;66:213–221.
28. Buchwald G, van der Stoop P, Weichenrieder O, Perrakis A, van Lohuizen M, Sixma TK. Structure and E3-ligase activity of the ring-ring complex of polycomb proteins bmi1 and ring1b. EMBO J 2006;25:2465–2474.
29. Afonine PV, Grosse-Kunstleve RW, Echols N, Headd JJ, Moriarty NW, Mustyakimov M, Terwilliger TC, Urzhumtsev A, Zwart PH, Adams PD. Towards automated crystallographic structure refinement with phenix.refine. Acta Crystallogr D Biol Crystallogr 2012;68:352–367.
30. Emsley P, Cowtan K. Coot: model-building tools for molecular graphics. Acta Crystallogr D Biol Crystallogr 2004;60:2126–2132.
31. Arnold K, Bordoli L, Kopp J, Schwede T. The SWISS-MODEL workspace: a web-based environment for protein structure homology modelling. Bioinformatics 2006;22:195–201.
32. Ramachandran S, Kota P, Ding F, Dokholyan NV. Automated minimization of steric clashes in protein structures. Proteins 2011;79:261–270.
33. Krissinel E, Henrick K. Inference of macromolecular assemblies from crystalline state. J Mol Biol 2007;372:774–797.